Flexural Behavior of Preloaded RC Slabs Strengthened with Prestressed CFRP Laminates

Renata Kotynia[1]; Krzysztof Lasek[2]; and Michal Staskiewicz[3]

Abstract: Many studies performed on reinforced concrete (RC) members strengthened in flexure with externally bonded (EB) fiber-reinforced polymers (FRPs) have indicated quite low strengthening efficiency caused by debonding of the FRP from the concrete surface prior to the capacity of the FRP material being achieved. It should be emphasized that although flexural strengthening with FPR increases the load-bearing capacity of RC members, it has little effect on the serviceability limit state (i.e., cracking moment and deflections). Prestressing the EB FRP has been proposed as a method of increasing utilization of the FRP tensile strength and of improving the efficiency of strengthening in terms of serviceability limit states. An experimental research program consisting of three series of RC slabs with variations in the longitudinal steel reinforcement ratio, concrete strength, preloading level before strengthening, and adhesion between the CFRP laminates and the concrete is described. A practical and unique aspect of the program focuses on an analysis of the effect of preloading on the strengthening efficiency of RC slabs strengthened with prestressed carbon fiber-reinforced polymer (CFRP) laminates. Although the preloading is one of the most important parameters to be accounted for in the design of strengthening existing RC structures, this aspect has been investigated only rarely. Two levels of slabs preloading were considered: the slab self-weight acting alone and the self-weight plus an additional external load. The self-weight preloading level corresponded to 25 and 14% of the yield strength of nonstrengthened slabs in Series I and III, respectively. The higher preloading level, equal to 76% of the yield strength of the nonstrengthened slab, was chosen to approach the elastic limit of the slab behavior. Experimental tests yielded promising results for the ultimate and serviceability limit states of the strengthened slabs. The strengthening ratio, defined as the ratio of the difference between the ultimate load of the strengthened and nonstrengthened slabs to the ultimate load of the nonstrengthened slab, reached values in the range of 0.64–1.19. The influence of the tensile steel reinforcement ratio, adhesion between the prestressed CFRP laminate and concrete, and preloading level on the ultimate load carrying capacity following strengthening is discussed. **DOI: 10.1061/(ASCE)CC.1943-5614.0000421.**

Author keywords: Carbon fibre reinforced polymer (CFRP) laminate; Prestressing; Strengthening; Reinforced concrete slab; Failure; Debonding.

Introduction

Common techniques for strengthening reinforced concrete (RC) members in flexure include externally bonded (EB) fiber-reinforced polymer (FRP) laminates/sheets on the tensile concrete surface and near-surface mounted (NSM) strips/bars glued into slots made in the concrete cover. Although EB carbon fiber-reinforced polymer (CFRP) has been widely used for the flexural strengthening of existing RC structures, studies have indicated the low efficiency of this technique resulting from intermediate crack debonding (IC) from the concrete surface limiting the CFRP material strength that can be developed. Strain utilization of EB CFRP typically ranges from 30 to 35% of the tensile strength (Kotynia et al. 2008) while NSM CFRP can achieve as high as 80% (Kotynia 2006).

It has been shown that although EB CFRP increases the load-bearing capacity of RC members, they do not significantly affect the cracking load and deflections under service loads. Prestressing the CFRP prior to bonding to the concrete surface is one of the best techniques to improve the serviceability of FRP-strengthened structures. The prestressing effectively reduces crack widths, relieves stress in the internal reinforcement, controls the crack distribution, limits deflection, and increases the load-carrying capacity of RC members (Deuring 1993; Triantafillou et al. 1992; Meier 1995; Wight et al. 2001).

The main challenge of strengthening RC structures with prestressed CFRP is proper anchorage of the CFRP terminations. To overcome the significant shear stress in the area where the tensile force is transferred from the laminate to the concrete, mechanical anchorage with steel plates is usually applied (Wight et al. 2001; El-Hacha et al. 2003; Kim et al. 2008). Such anchorage introduces a mechanical clamping of the laminate to promote a more ductile failure mode and to permit a higher prestressing level of the CFRP laminate (El-Hacha et al. 2003). An innovative, nonmechanical anchorage method proposed by Stöcklin and Meier (2003) was developed and successfully tested (Czaderski and Motavalli 2007; Aram et al. 2008; Kotynia et al. 2011). Young-Chan et al. (2012) recently described a revised prestressing system for flexural strengthening with CFRP laminates and sheets. Failure of flexural members strengthened with mechanically anchored CFRP laminates may occur in two modes: two-stage debonding followed by CFRP rupture or sudden CFRP rupture.

Review of available literature on strengthening of RC members with prestressed laminates shows that the strengthening effect significantly depends on a number of factors, including the type of

[1]Associate Professor, Dept. of Concrete Structures, Lodz Univ. of Technology, Al. Politechniki 6, 90-924 Lodz, Poland (corresponding author). E-mail: renata.kotynia@p.lodz.pl

[2]Ph.D. Student, Dept. of Concrete Structures, Lodz Univ. of Technology, Lodz, Poland. E-mail: krzysztof.lasek@p.lodz.pl

[3]Ph.D. Student, Dept. of Concrete Structures, Lodz Univ. of Technology, Lodz, Poland. E-mail: michal.staskiewicz@p.lodz.pl

Note. This manuscript was submitted on March 19, 2013; approved on July 22, 2013; published online on July 24, 2013. Discussion period open until December 24, 2013; separate discussions must be submitted for individual papers. This paper is part of the ***Journal of Composites for Construction***, © ASCE, ISSN 1090-0268/(0)/$25.00.

laminate, its stiffness, the number of layers, and the existing longitudinal and shear reinforcement ratios (Teng et al. 2002). Many researchers have shown that application of prestressed CFRP laminates can increase the ultimate load-carrying capacity by up to 170% (Young-Chan et al. 2012; Kim et al. 2008; Pellegrino and Modena 2009; Yu et al. 2008; Kałuża and Ajdukiewicz 2008; Wight et al. 2001). Nonprestressed CFRP strengthening is able to achieve increases of ultimate load-carrying capacity up to 40% (Kotynia and Kamińska 2003). Test on RC slabs (or flat beams) strengthened with prestressed FRP account for only about 10% of available test data. One of the most detailed researches carried out on RC slabs considered seven RC slabs ($6{,}500 \times 1{,}000 \times 220$ mm) tested in 4-point bending under monotonic (four slabs) and cyclic loading (three slabs) (Stöcklin and Meier 2003; Kotynia et al. 2011). Monotonic test results indicated that the slabs strengthened with prestressed CFRP laminates achieved a cracking load about 65% higher than that of a nonstrengthened control. The ultimate load-carrying capacity was increased from the control by 66% using prestressed CFRP and only by 26% using nonprestressed CFRP.

Experimental Program

A practical and unique goal of the reported test program focuses on an analysis of the effect of preloading on the strengthened behavior of RC slabs strengthened with prestressed CFRP laminates. Although preloading is one of the most important parameters to be taken into account in the design of strengthening existing RC structures, based to the authors' knowledge, this aspect has been investigated only very rarely. The self-weight of RC beams represents a relatively small contribution to beam load; however, for slabs the self-weight may represent a significant portion of the member capacity, particularly where relatively low reinforcing ratios are used. For this reason, the primary parameter investigated in this research was the level of slab preloading prior to and during strengthening. The slabs were strengthened under two preloading levels. The lower preloading level was equal the self-weight of the slabs only; this corresponded to 25 and 14% of the yield strength of nonstrengthened slabs in Series I and III, respectively (the difference was caused by each series having a different steel reinforcement ratio). The higher preloading level, 76% of the yield strength of the nonstrengthened member, was selected to approach the elastic limit of the unstrengthened slab behavior. To reflect the variability seen in existing structures, the longitudinal reinforcement ratio of the test slabs was varied by using two different bar diameters: 12 and 16 mm. Adhesion between the prestressed CFRP and the concrete was also considered in this study. Most of the slabs in the experimental program were strengthened with prestressed CFRP laminates bonded to the concrete with epoxy adhesive. Two slabs, however, were strengthened without any adhesive between the laminates and the concrete; the laminates behaved like an external bowstring attached to the slab only at the anchorage plates. An "a" index in the slab identification indicates the presence of adhesive. Finally, in one slab, the mechanical anchorage system was removed following the prestressed CFRP being bonded to the concrete. A summary of all the investigated parameters is shown in Table 1. The slabs were given the following designations: B12 and B16 = slabs reinforced with 12 and 16 mm longitudinal steel bars, respectively, a = presence of adhesive, sp = presence of steel plates anchorage system, and e = preloading with the external load before and during strengthening.

Test Specimens

All the tests were performed in the laboratory of the Department of Concrete Structures at Lodz University of Technology. The experimental program has the same test spans, slab depth, and loading arrangement as the previously successful EMPA study conducted by Stöcklin and Meier (2003). The slab width is one-half that tested at EMPA and only a single prestressed CFRP laminate is used in the present study. The experimental program consisted of three series of slabs (I, II, and III), which contained seven 500×220 mm RC slabs in total. Series I and II together included five slabs reinforced with four 12-mm-diameter bars in tension. Series III contained two slabs reinforced with four 16-mm-diameter bars. All the slabs were reinforced with four 8-mm-diameter bars in the compression zone. The shear reinforcement consisted of 8-mm-diameter steel stirrups with a 150-mm spacing. The concrete cover in all slabs was 25 mm. Each 500- $\times$ 220-mm slab was tested in six-point loading over a 6,000-mm simple span. Specimen details are shown in Fig. 1.

Material Properties

The slabs were cast on three different dates with commercially supplied Class C30/37 concrete. The average compressive strength (f_c) and modulus of elasticity (E_c), defined from uniaxial compression tests of 150×300-mm cylinders in addition to the compression and tension strengths determined from 150 mm cubes, are summarized in Table 2. The uniaxial tensile characteristics of steel bars used for the reinforcing of slabs in Series I, II, and III are shown in Table 3. The 5% yield strength differences of the 12-mm bars did not significantly influence the behavior of the slabs. The average tensile strength (f_{fu}), elastic modulus (E_f), and ultimate strain (ε_{fu}) values of the CFRPs are also presented in Table 3. Differences between strength characteristics for the same reinforcing steel diameters (8 mm or 12 mm) resulted from the steel coming from different heats. The yield strengths of the 12-mm bars varied approximately 5% and, therefore, did not significantly influence the behavior of the slabs. The 8-mm bars were used for shear reinforcement only, and, therefore, did not affect the flexural behavior of the slabs. The 100×1.2-mm CFRP strips were bonded to the slabs using S&P Resin 55 epoxy adhesive. The components of the

Table 1. Summary of Parameters Investigated

Series	Slab	Tensile steel reinforcement	Anchorage technique	Preloading	$2F_p$ (kN)	$2F_p/2F_{u0}$
I	B12-asp	4#12	Adhesive+steel plate	Self-weight only	6.3[a]	0.25
	B12-sp	4#12	Steel plate	Self-weight only	6.3[a]	0.25
II	B12-asp-e	4#12	Adhesive+steel plate	Self-weight + $2F_p$ = 13.7 kN external load	20.0	0.76
	B12-sp-e	4#12	Steel plate	Self-weight + $2F_p$ = 13.7 kN external load	20.0	0.76
	B12-a	4#12	Adhesive	Self-weight only	6.3[a]	0.25
III	B16-asp	4#16	Adhesive + steel plate	Self-weight only	6.3[a]	0.14
	B16-asp-e	4#16	Adhesive + steel plate	Self-weight + $2F_p$ = 27.5kN external load	33.8	0.76

[a]Equivalent representation of slab self-weight: $2F_p$ = preload load; $2F_p/2F_{u0}$ = preloading ratio.

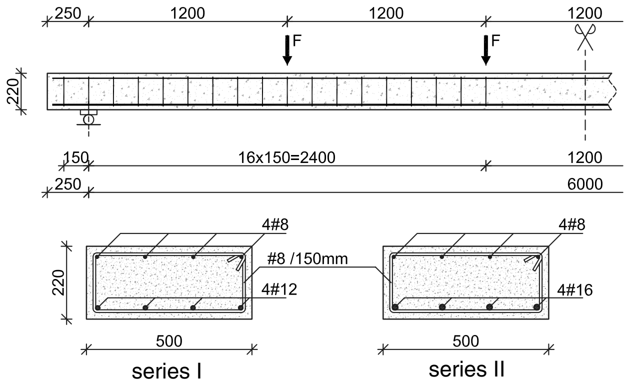

Fig. 1. Test specimen geometry, details, and loading arrangement (dimensions in mm)

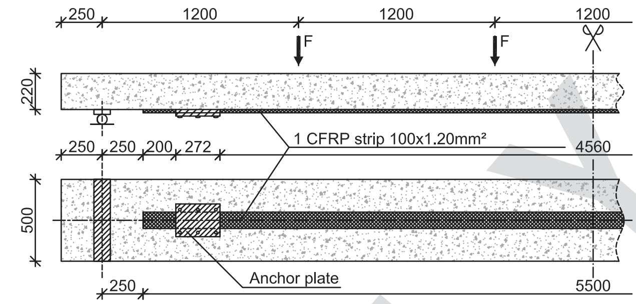

Fig. 2. Strengthening mode of slabs (dimensions in mm)

Table 2. Strength Characteristics of Concrete

Slab	Series	Age (days)	$f_{c.\mathrm{cube}}$ (MPa)	$f_{ct,sp}$ (MPa)	f_c (MPa)	E_c (GPa)
B12-asp	I	266	35.3	2.65	32.2	23.7
B12-sp	I	311	33.8	3.13	28.7	24.7
B12-asp-e	II	55	44.0	3.50	41.6	24.7
B12-sp-e	II	77	46.7	3.48	40.9	25.4
B12-a	II	198	50.3	3.60	45.3	24.3
B16-asp	III	61	52.4	3.65	49.0	25.4
B16-asp-e	III	71	60.3	5.30	51.0	26.4

Table 3. Strength Characteristics of Steel and CFRP Laminate

Material	A_s (mm^2)	f_y (MPa)	f_t or f_{fu} (MPa)	E_s or E_f (GPa)	ε_{fu}
Series I					
Steel bar #8	48.9	583.1	650.5	200.7	—
Steel bar #12	111.0	511.4	594.5	191.1	—
Series II					
Steel bar #8	49.4	416.2	734.1	186.1	—
Steel bar #12	113.3	539.6	627.5	191.3	—
Series III					
Steel bar #8	48.8	555.8	646.0	196.4	—
Steel bar #16	199.1	595.0	672.0	198.0	—
CFRP laminate	—	—	2,857	173.3	0.0168

adhesive were mixed in 3:1 proportions (epoxy to hardener, by weight). The average tensile strength in bending ($f_{ct,fl}$) and the compressive strength (f_c) were experimentally determined from standard prisms to be equal to 23.2 and 57.9 MPa, respectively.

Strengthening Techniques

Each RC slab was strengthened with a single 100 × 1.2-mm prestressed CFRP strip as shown in Fig. 2. The initial CFRP prestressing strain obtained using the S&P prestressing system was intended to be equal to 0.005, corresponding to 30% of the CFRP tensile strength. In fact, there were slight differences of the applied prestressing strain values, varying from 0.0044 to 0.0052. The measured prestressing losses did not exceed 8% of the assumed strain value (0.005). The slabs were strengthened in situ in the test frame with laminates bonded to the concrete using a two-part epoxy adhesive. Prior to strengthening, the bottom surface of the slab was prepared by removing the thin, superficial cement paste layer. After preparing the concrete surface, steel bolts were installed on the bottom of the slab for the steel-plate anchorage system. The slabs were strengthened under loading (consisting of the dead load and/or external load as indicated in Table 1). After the CFRP laminates were mounted in the anchorage system, a hydraulic jack was installed at the stressing (active) end in order to prestress the CFRP. The prestress force was anchored and blocked and the CFRP adhesively bonded to the concrete along the full length between the anchors. The anchors remain in place during testing (in all but one slab) but the blocking was removed after 12 h. Two of the seven slabs (B12-sp and B12-sp-e) were strengthened without the CFRP being bonded along the slab length between anchors; in these slabs, the prestressing force was transferred only at the anchorage locations. Slab B12-a was strengthened using the same system but with a reduction in the prestressing force at the end of the laminate. The CFRP was prestressed and bonded to the concrete over only the middle 3,600 mm of the slab, leaving 1,000 mm adjacent each anchorage unbonded. After 72 h, mechanical grips were installed at both ends of the bonded section of the laminate, pressing it to the concrete surface to prevent CFRP debonding. The steel plates of the anchorage system were removed and the remaining 1,000 mm long, nonprestressed sections were bonded to the concrete surface without any prestressing force. After another 72 h, the mechanical grips were removed, and the laminate remained without any anchors.

Test Set-Up and Protocol

The slabs were simply supported on steel hinges and placed on concrete blocks [Fig. 3(a)]. All the slabs were subjected to six-point monotonic loading and introduced by two hydraulic jacks with a maximum capacity of 100 kN each. The force from each of the jacks was transferred to the concrete member through a steel spreader supported at two points on the slab [Fig. 3(b)]. Each specimen was tested until failure. To facilitate direct comparison of all specimens, the slab self-weight is included in all load values as the equivalent load located at the loading points. That is, $2F_p = 6.3$ kN (Table 1) is not an applied load but is the equivalent representation of the slab self-weight.

All slabs were initially loaded to their prescribed load ($2F_p$ in Table 1). In the case of Slabs B12-asp and B12-sp, the unloading-loading process was cycled six times to evaluate the plastic deformation of the slabs after their strengthening. Following appropriate CFRP cure, the applied load was increased monotonically to failure of the strengthened slab.

To evaluate the slab deflection, nine 50-mm LVDTs were placed at midspan and at either side of each load point, as shown in Fig. 4(a). Concrete strains in the tension (13 gauges) and compression (5 gauges) zones were measured using 10- or 20-mm LVDTs

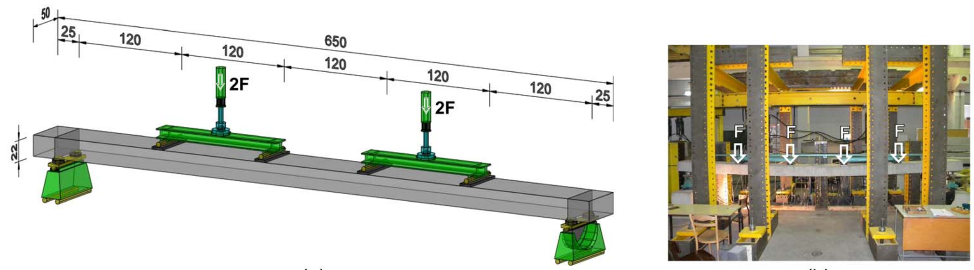

(a) (b)

Fig. 3. Test set-up (dimensions in mm)

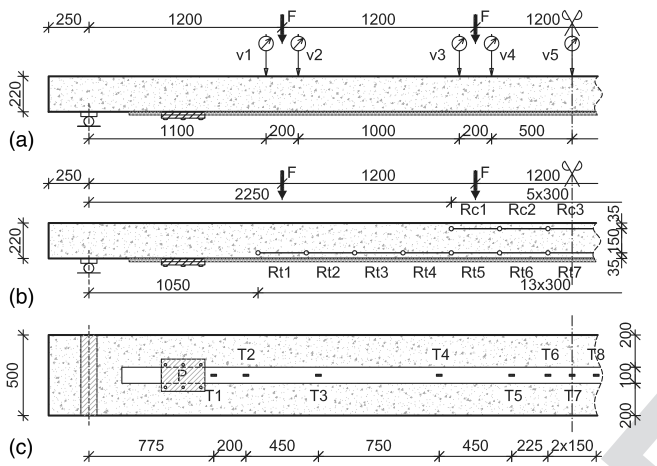

Fig. 4. Location of gauges: (a) LVDTs for vertical displacement measurements; (b) LVDTs for concrete strain measurements; (c) strain gauges on CFRP laminate (dimensions in mm)

Fig. 5. View of slab after primary failure due to CFRP debonding showing the "fish bone" crack pattern on the bottom of the slab

Fig. 6. View of the secondary failure due to sliding of the CFRP laminate under the anchor plate

arranged over 300-mm gauge lengths as shown in Fig. 4(b). CFRP strains were recorded from strain gauges located at several points along the length of the laminate as indicated in Fig. 4(c). Loads were obtained from load cells at the actuators (thus, $2F$ is recorded) and the self-weight, $2F = 6.3$ kN added. All sensors were connected to a data acquisition device connected to PC Lab software.

Analysis of Tests Results

Failure Modes

The most common failure mode, observed in all RC slabs strengthened with the CFRP laminates bonded along their entire length (B12-asp, B12-asp-e, B16-asp, B16-asp-e, and B12-a), was an intermediate crack-induced (IC) debonding of the CFRP laminate initiating at one of the middle loading points and extending toward the near support (Fig. 5). A secondary failure, occurring after IC debonding, was the CFRP sliding from under the anchorage plate (Fig. 6). Anchorage slip was also the primary failure mode of Specimen B12-sp-e (strengthened without bonding the CFRP laminate). After CFRP debonding, the "fishbone" crack pattern, typical of IC debonding, was evident on the bottom concrete surface of the slabs (Fig. 5). A concrete crushing failure was observed in only one slab, B12-sp (Fig. 7). The ultimate loads (F_u), initial CFRP prestressing strains (ε_{fp}) and corresponding stresses (σ_{fp}), and maximum observed CFRP strains ($\varepsilon_{f,\text{test}}$) are shown in Table 4.

Crack Pattern

Maps of cracks after failure of four selected slabs from Series I and III are shown in Fig. 8. In general, the crack patterns are similar in all the tested slabs. Minor differences were caused by the preloading effect and the absence of adhesive. Slab B12-asp-e strengthened under a high-preloading level of 76% of the yield strength exhibited more vertical cracks both in the bending and in the support region.

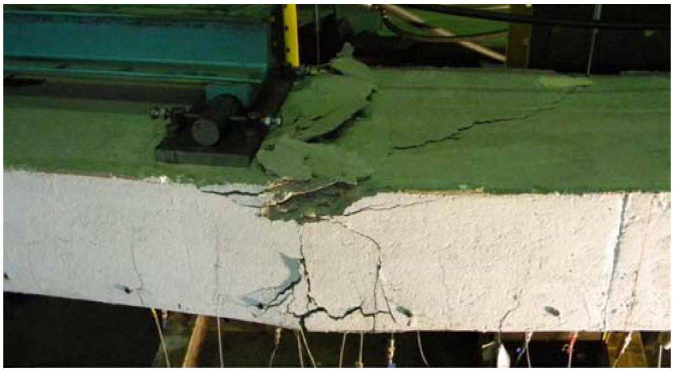

Fig. 7. Concrete crushing in compression zone

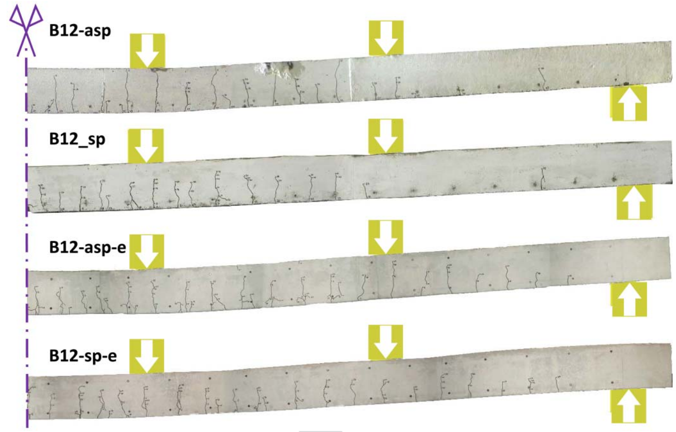

Fig. 8. Crack patterns in the slabs of Series I and II

The strengthening of the comparable Slab B12-asp at a lower preload (25% of yield) led to an earlier contribution of the CFRP in resisting tensile forces resulting in improved crack control and mitigation of crack development in the support region. This observation was confirmed in the tests of comparable Slabs B12-sp and B12-sp-e. In all cases, the concrete crack width increased until IC debonding initiated at a critical crack. There were no significant differences in the crack patterns of slabs strengthened under the lower preload having bonded or unbonded laminates (B12-asp, B12-sp).

CFRP Strains

CFRP strains resulting from applied loads reached higher values for slabs strengthened with bonded laminates than those strengthened without CFRP bonding. The maximum load-induced strain ($\varepsilon_{f,\text{test}}$) observed for the unbonded laminates indicated values of 0.0069 for Slab B12-sp and 0.0050 for Slab B12-sp-e, while the bonded laminates of Slabs B12-asp and B12-asp-e reached strains of 0.0093 and 0.0069, respectively. The initial preloading of the slabs to $0.76F_{u0}$ resulted in a lower maximum load-induced CFRP strain compared with the slabs preloaded with $0.25F_{u0}$ or $0.14F_{u0}$. This effect is demonstrated by the CFRP strains for the slabs in both Series I and II (B12-asp and B12-asp-e, mentioned earlier) and in Series III, where the high preloading caused a decrease in the load-induced CFRP strain at failure from 0.0080 in Slab B16-asp to 0.0072 in Slab B16-asp-e. The removal of the anchor plates (Slab B12-a) resulted in a lower load-induced CFRP strain at debonding, $\varepsilon_{f,\text{test}} = 0.0064$, compared to Slab B12-asp with the laminate anchored at the ends which exhibited $\varepsilon_{f,\text{test}} = 0.0093$. The other reasons for a lower CFRP strain at debonding in Slab B12-a was the stepped prestressing force in the laminate as it transitions from the prestressed to nonprestressed regions along the length of the laminate.

The total CFRP strain is calculated as the sum of the CFRP prestressing strain and the maximum load-induced strain observed during the test (i.e., $\varepsilon_{f,\text{tot}} = \varepsilon_{fp} + \varepsilon_{f,\text{test}}$). Fig. 9 shows the total CFRP strain distribution along the length of the laminate, at different loading stages of Slab B12-asp-e. It is clearly seen that the CFRP at the location of the load immediately to the right of midspan is bonded at $2F = 46$ kN (curve "A"). IC debonding initiated under the load at $2F = 48$ kN and propagated toward the right support (curve "B"). Shortly thereafter (still at $2F = 48$ kN), local debonding occurred under the load to the left of midspan and propagated toward the left support (curve "C"). After the laminate debonded along it full length, it was held only by the anchor plates and behaved as an external bowstring (evident as the relatively uniform strain distribution of curve "C" in Fig. 9), until failure of the anchorage system.

Concrete Strains in Tensile Zone

Comparisons of the average concrete tensile strain at the level of the steel reinforcement [$\varepsilon_{t,\text{aver}}$, derived from measurements of Sensors Rt6, Rt7, and Rt8, see Fig. 4(b)] as a function of the applied load

Table 4. Summary of Test Results

Slab	$2F_{u0}$ (kN)	$2F_p$ (kN)	$2F_p/2F_{u0}$	$2F_u$ (kN)	η_F	ε_{fp}	σ_{fp} (MPa)	$\varepsilon_{f,\text{test}}$	$\eta_{\varepsilon f}$	Failure mode
B12-asp	24	6.3	0.25	52.6	1.19	0.0052	900 $0.32f_{fu}$	0.0093	0.87	CFRP debonding; strip's end sliding from anchorage system
B12-sp	24	6.3	0.25	46.8	0.95	0.0046	796 $0.28f_{fu}$	0.0069	0.68	Concrete crushing
B12-asp-e	26	20.0	0.76	48.3	0.86	0.0048	822 $0.29f_{fu}$	0.0068	0.69	CFRP debonding; strip's end sliding from anchorage system
B12-sp-e	26	20.0	0.76	45.1	0.73	0.0044	762 $0.27f_{fu}$	0.0050	0.56	CFRP end sliding from anchorage system
B12-a	26	6.3	0.25	50.6	0.94	0.0051	885 $0.30f_{fu}$	0.0064	0.68	CFRP debonding
B16-asp	44	6.3	0.14	74.4	0.69	0.0048	831 $0.29f_{fu}$	0.0080	0.76	CFRP debonding; strip's end sliding from anchorage system
B16-asp-e	44	33.8	0.76	72.0	0.64	0.0048	840 $0.29f_{fu}$	0.0072	0.71	CFRP debonding; strip's end sliding from anchorage system

Note: η_F—strengthening ratio, $\eta_F = (F_u - F_{u0})/F_{u0}$; $\eta_{\varepsilon f}$—strain efficiency, $\eta_{\varepsilon f} = (\varepsilon_{fp} + \varepsilon_{f,\text{test}})/\varepsilon_{fu}$; and $\varepsilon_{f,\text{test}}$—maximum applied load-induced tensile strain of CFRP laminate registered at slab failure.

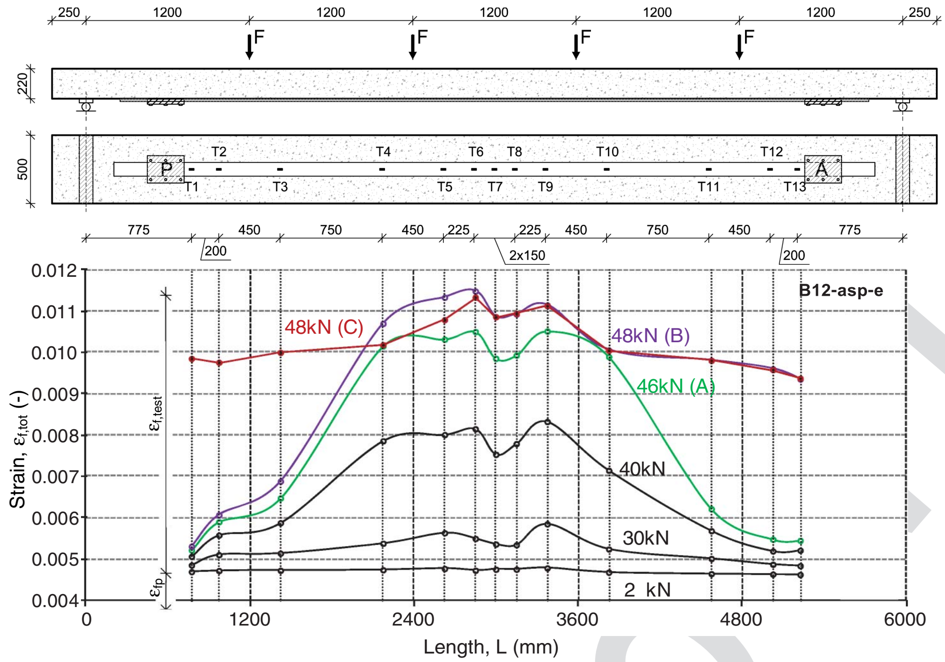

Fig. 9. CFRP strain along Slab B12-asp-e (dimensions in mm)

are shown in Figs. 10–12. These figures show the test results of the slabs of Series I and II strengthened with laminates bonded to the concrete (B12-asp, B12-asp-e, and B12-a), slabs having unbonded laminates (B12-sp and B12-sp-e), and slabs of Series III (B16-asp-e), respectively. Such a comparison of all slabs clearly shows the influence of the high preload on the behavior of the strengthened slabs (comparison of Slabs B12-asp and B12-asp-e, B12-sp and B12-sp-e, and B16-asp and B16-asp-e). Although the slabs having a higher preload had a higher concrete strains for the same load than corresponding slabs having a lower preload level (concrete strains are 14 and 10% greater for the beams of Series I, II, and III, respectively, as shown in Figs. 10 and 12), there was an undeniable strength increase for all the slabs and the strengthening allowed the slabs to regain their stiffness despite the high-level preloading virtually exhausting the slabs' elastic capacity. In general, the preloading level did not affect the ultimate concrete tensile strains. A comparison of the concrete tensile strain versus load curves (Figs. 10 and 11) confirms a significant beneficial effect of providing adhesive between the laminates and the concrete. Larger concrete tensile strains occurred in the slabs strengthened with the unbonded laminates (Fig. 11) than in the slabs strengthened with bonded laminates (Fig. 10). The different loading history of Slabs B12-asp and B12-sp (due to the unloading and reloading process, see Figs. 10 and 11) did not affect the flexural behavior of these slabs after strengthening.

Vertical Displacements

The vertical displacements indicated that all the slabs deformed symmetrically in relation to their midspan. An example of displacements profiles for selected load levels for Slab B16-asp-e is shown in Fig. 13. The two lower most curves ("C" and "D") corresponding to deflections under the load of $2F = 72$ kN are drawn with a dashed line because four measurements (V3, V4, V8, and V9) were not recorded at this loading stage. In these cases, the midspan deflection was recorded with a ruler.

The influence of adhesion between the CFRP and the concrete on the midspan vertical displacement of Slabs B12-asp, B12-sp, and B12-a is shown in Fig. 14(a). When the longitudinal steel reinforcement begins to yield, the deflection of the slab with unbonded laminates (B12-sp) is noticeably higher than that of the slabs strengthened with bonded laminates (B12-asp). The same

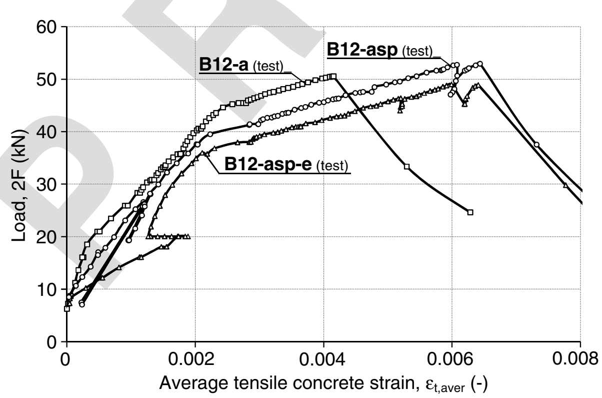

Fig. 10. Average concrete tensile strains in the slabs of Series I and II (with adhesive)

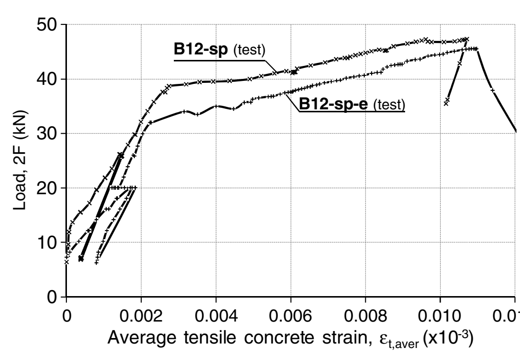

Fig. 11. Average concrete tensile strains in the slabs of Series I and II (without adhesive)

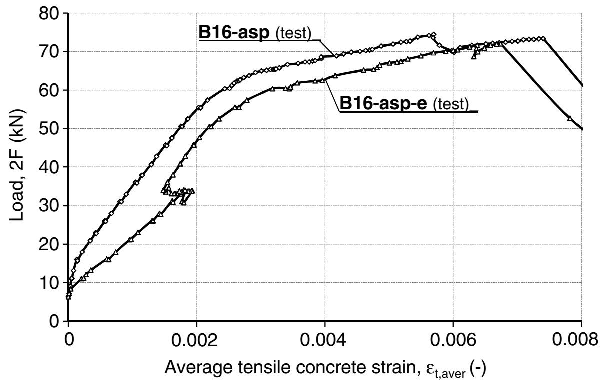

F12:1 **Fig. 12.** Average concrete tensile strains in the slabs of Series III

observation was made for Slabs B12-asp-e (bonded) and B12-sp-e (unbonded) that were subject to higher preloads before strengthening [Fig. 14(b)]. This result demonstrates that the slabs strengthened with unbonded laminates have lower stiffness after the steel yields, when the CFRP contribution to the transference of tensile forces significantly increases. Moreover, Fig. 14(c) confirms the negligible effect of preloading (even at high levels) on the deflection of the strengthened slab; both Slabs B16-asp-e and B16-asp reached similar maximum deflections [Fig. 14(c)].

Strengthening Ratio and CFRP Strain Efficiency

The results of the tests were evaluated using a strengthening ratio (η_F), defined as the ratio of the increase in the ultimate load resulting from strengthening ($F_u - F_{u0}$) to the ultimate load of the unstrengthened slab (F_{u0}):

$$\eta_F = (F_u - F_{u0})/F_{u0} \tag{1}$$

The capacity of the unstrengthened slab, F_{u0}, was determined analytically using the approach described in the next section. The test results summarized in Table 4 illustrate the influence of the variable parameters on the strengthening ratio. The slabs of Series I and II, having a lower reinforcement ratio, achieved a higher strengthening ratio (from 0.86 to 1.19) than the slabs of Series III (from 0.64 to 0.69). Additionally, the slabs with bonded CFRP laminates (B12-asp and B12-asp-e) achieved higher reinforcement

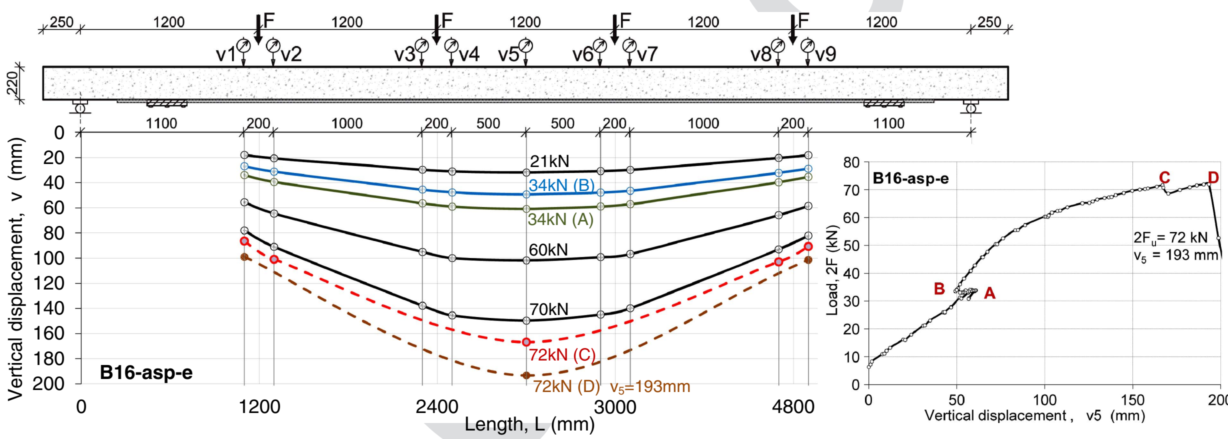

F13:1 **Fig. 13.** Vertical displacement of Slab B16-asp-e (dimensions in mm)

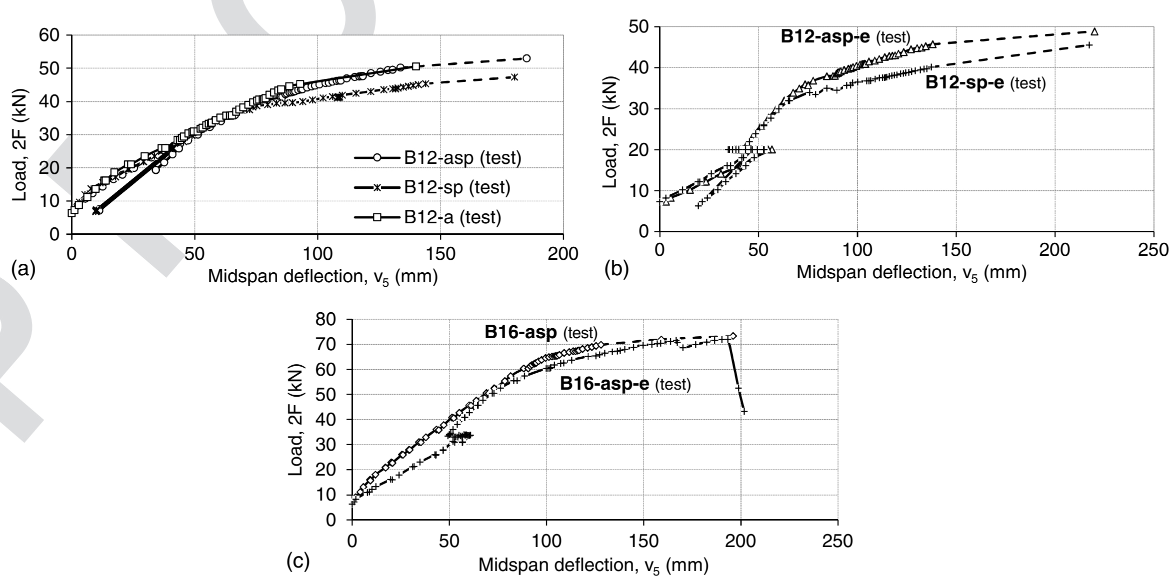

F14:1 **Fig. 14.** Comparison of midspan displacements of slabs: (a) B12-asp, B12-sp, and B12-a; (b) B12-asp-e and B12-sp-e; (c) B16-asp and B16-asp-e ratios than corresponding slabs with unbonded laminates (B12-sp and B12-sp-e). High-preloading levels resulted in a decrease in the strengthening ratio. Specifically for Slab B12-sp, strengthened under a preload of $0.25F_{u0}$, a strengthening ratio of 0.95 was achieved; for Slab B12-sp-e, strengthened under a preload of $0.76F_{u0}$, the strengthening ratio was 0.73.

The strain efficiency of the CFRP laminate, a measure of the degree of utilization of its tensile strength, is defined as the ratio of the total strain at debonding (i.e., usable strain) of the laminate to the CFRP ultimate strain capacity:

$$\eta_{\varepsilon f} = \varepsilon_{f,\mathrm{tot}}/\varepsilon_{fu} \tag{2}$$

In general, the slabs exhibiting higher CFRP prestressing strain (ε_{fp}) achieved higher CFRP strain efficiency. Slab B12-asp, strengthened with the laminate initially prestressed to a strain of 0.0052, reached the highest strengthening ratio of $\eta_F = 1.19$ and the highest CFRP strain efficiency of $\eta_{\varepsilon f} = 0.87$ (Table 4). Similar to the strengthening ratio, CFRP strain efficiency is positively influenced by the presence of adhesive over the full length of the CFRP strips. Slabs strengthened with unbonded CFRP achieved strain efficiency ratios of 0.68 (B12-sp) and 0.56 (B12-sp-e), while the corresponding slabs strengthened with bonded laminates reached strain efficiency ratios of 0.87 (B12-asp) and 0.69 (B12-asp-e). CFRP strain efficiency of the slabs having large preloads before strengthening (B12-asp-e and B12-sp-e) was lower (0.69 and 0.56) than of those strengthened under lower preload levels (0.87 for B12-asp and 0.68 for B12-sp).

Analytical Model

For comparison of calculated and test results, a nonlinear model for RC members (Czkwianianc and Kaminska 1993) was adapted to include strengthening with prestressed FRP laminates. The model considers only normal stresses in the section and that initially plane sections remain plane [Fig. 15(a)]; thus, strain compatibility is enforced in the cross section. A nonlinear stress-strain (σ-ε) relationship for concrete compression and tension is adopted [Fig. 15(b)]. This relationship is defined as a function of concrete strength and the rate at which strain is applied as follows:

$$\sigma_c = f_c \frac{\beta \frac{\varepsilon_c}{\varepsilon_{c1}}}{\beta - 1 + (\frac{\varepsilon_c}{\varepsilon_{c1}})^{\beta}} \tag{3}$$

$$\beta = \frac{1}{1 - \frac{f_c}{\varepsilon_{c1} E_c}} \tag{4}$$

$$E_c = E_{c0}[0.99 - 0.0158 \ln(t_m) - 0.0013 f_{c,\mathrm{cube}}] \tag{5}$$

$$E_{c0} = 4.03 \times (2300 + 3.17 f_{c,\mathrm{cube}}) f_{c,\mathrm{cube}}^{1/3} \tag{6}$$

$$\varepsilon_{c1} = [0.0075 f_{c,\mathrm{cube}} + 0.125 \ln(t_m) + 1.655] \times 10^{-3} \tag{7}$$

$$\varepsilon_{cu} = [4.51 - 0.1244 f_{c,\mathrm{cube}} + 0.000948 f_{c,\mathrm{cube}}^2 t_m^{0.14} + 2.20] \times 10^{-3} \tag{8}$$

$$f_c = [0.83 - 0.01 \ln(t_m)] f_{c,\mathrm{cube}} \tag{9}$$

$$f_{cu} = (0.0051 f_{c,\mathrm{cube}} + 0.38) f_{c,\mathrm{cube}} \tag{10}$$

where E_c = elasticity modulus of concrete; f_c = compressive strength of concrete; f_{cu} = ultimate compressive strength of concrete; $f_{c,\mathrm{cube}}$ = compressive strength of concrete on cubic specimens; and t_m = time of stress increase.

The adopted model includes the transfer of tensile stresses in cracked concrete (tension stiffening). Experimentally determined reinforcing steel [Fig. 15(c)] and CFRP (Table 3) material properties are adopted. The value of the external load is defined according to the equilibrium condition of generalized forces in the cross section [Fig. 15(a)]

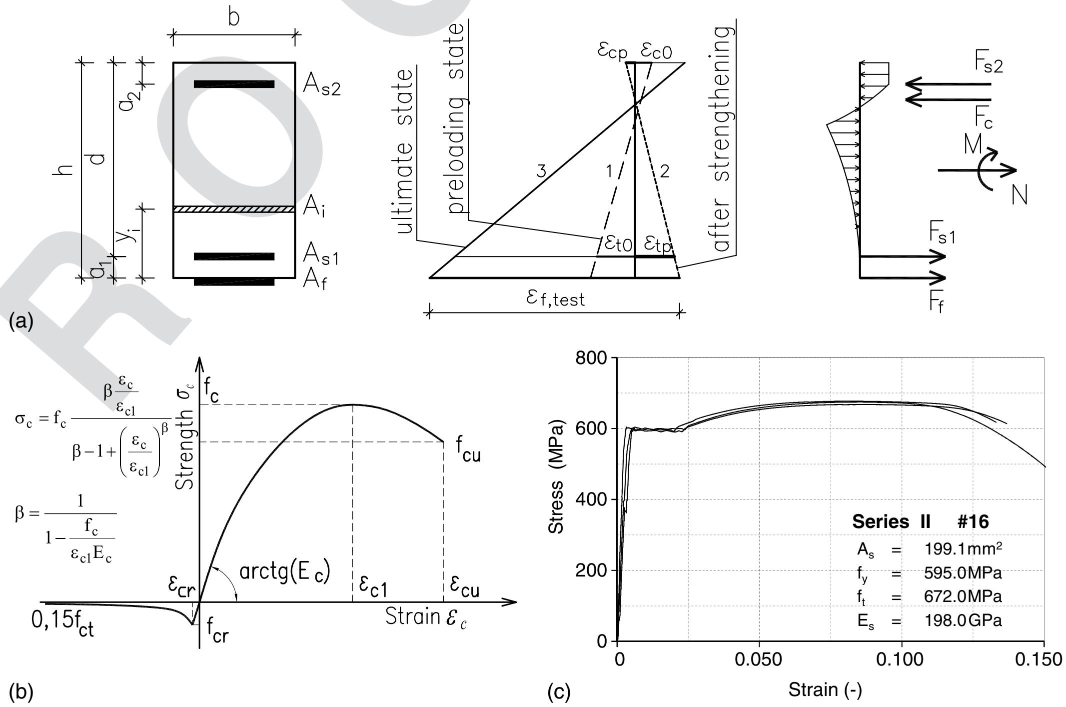

F15:1 **Fig. 15.** Calculation model: (a) plane cross-section principle; (b) stress-strain model of concrete; (c) stress-strain model of steel

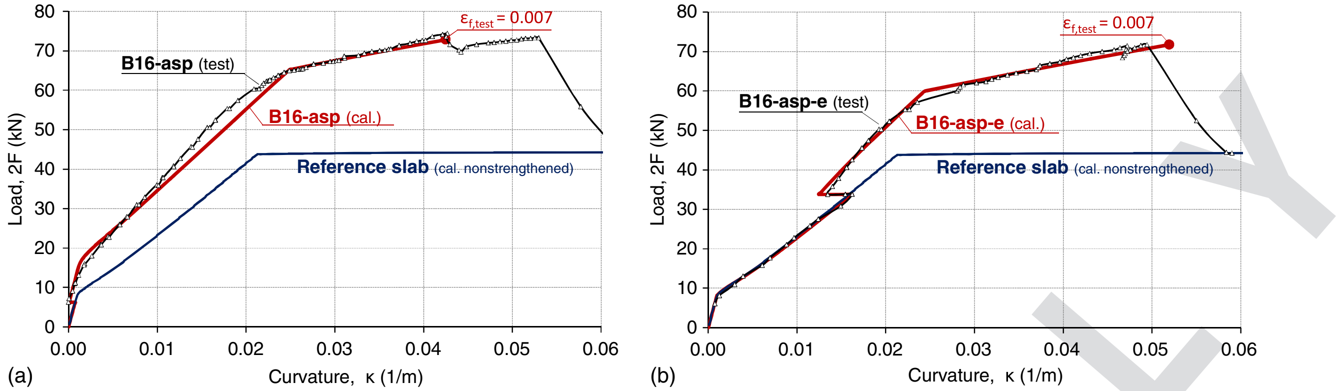

Fig. 16. Comparison of experimental and calculated curvatures for strengthened slabs and calculated responses for corresponding reference slabs: (a) B16-asp; (b) B16-asp-e

$$\sum_{i=1}^{n} F_i = N \quad \text{and} \quad \sum_{i=1}^{n} F_i y_i = M \tag{11}$$

The load-carrying capacity of the reference (unstrengthened) member is the load, determined from analysis, corresponding to state in which either the concrete compressive strain reaches $\varepsilon_{cu} = 0.0035$ or the steel strain reaches ε_{su} (ultimate tensile strain of steel reinforcement). IC debonding of the FRP laminate or CFRP rupture is considered to be additional expected failure modes for EB FRP strengthened members. Hence, the load-carrying capacity is calculated considering the additional CFRP debonding and rupture limit states defined as the CFRP strain achieving $\varepsilon_{f,\text{test}}$ (Table 4) or ε_{fu} (Table 3), respectively. The model has been successfully applied to the analytical verification of test results of unstrengthened RC slabs and RC beams and slabs externally strengthened with nonprestressed FRP laminates (Kotynia and Kaminska 2003).

It is a common engineering practice to consider the preloading state of RC members before strengthening. The greater the preload is in comparison to the member capacity before strengthening, the lower the increase in the load-carrying capacity and utilization of the CFRP laminate is expected to be. The initial loading state is considered in the analytical model with appropriate concrete strains and steel reinforcement strains equal to ε_{c0} and ε_{t0}, respectively [Fig. 15(a)]. The effect of adding prestressed CFRP is considered in the model by the addition of compressive and tensile strains in concrete (ε_{cp} and ε_{tp}) and in the CFRP strip (ε_{fp}). The most objective comparison of the experimental and calculated results is given by curvature (κ) calculated on the basis of the averaged concrete strains in the compression and tension zones, registered on the LVDTs located in the pure bending region [Fig. 4(b)], from the formula

$$\kappa = \frac{\varepsilon_t - \varepsilon_c}{h'} \, (1/\text{mm}) \tag{12}$$

where ε_t = average concrete strain in tension zone (with positive sign); ε_c = average concrete strain in compression zone (with negative sign); and h' = vertical distance between compressive and tensile strain measurements (mm).

Comparisons of experimental and calculated load-curvature responses ($2F$ versus κ) for the strengthened slabs of Series III (assuming the average CFRP strain $\varepsilon_{f,\text{test}} = 0.0070$) are shown in Fig. 16. Calculated load-curvature responses of the unstrengthened reference slab are also shown in Fig. 16. Both diagrams for the strengthened Slabs B16-asp and B16-asp-e validate the assumed analytical model over the entire range of loads. Therefore, this model is appropriate for the response prediction of EB FRP strengthened RC members flexural members strengthened with nonprestressed (passive) or prestressed (active) CFRP laminates, including the effects of preloading below the elastic limit prior to strengthening. Because the analytical approach makes the assumption of strain compatibility in the cross section, it is not directly applicable to the case of unbonded CFRP having only anchorage at the CFRP terminations. In such a case, the force from the unbonded CFRP may be considered as an externally applied load (limited by CFRP rupture) in the calculation of equilibrium.

Conclusions

To assess the effectiveness of flexural strengthening with prestressed CFRP laminates, three series of RC slabs with the same cross-sectional dimensions but with different longitudinal steel reinforcement, preloading levels, and with and without adhesion between laminates and concrete were tested under six-point loading. Each series was composed of slabs strengthened with prestressed CFRP laminates, either bonded or not bonded to the concrete. Slabs were preloaded and strengthened under the slab self-weight acting alone (approximately 25 or 14% of the yield strength of the unstrengthened slabs in Series I and III, respectively) and under the effect of external loading equal to approximately 76% of the yield strength of the unstrengthened slab. From the test results, the following conclusions are drawn:

- The most common failure mode observed in the test slabs was CFRP IC debonding. Slip of the CFRP end from under the anchorage plates was a secondary failure mode.
- The crack patterns were similar in all tested slabs. Minor differences were caused by the effect of preloading and the presence or absence of adhesive. The slabs having a high preload prior to strengthening indicated slightly more vertical cracking both in the span and near the support region.
- The high efficiency of the prestressing technique for flexural strengthening with EB CFRP laminates was confirmed by the strengthening ratio (η_F), which ranged from 0.68 to 1.19 for the beams of Series I and II (with lower steel reinforcement ratio) and from 0.64 to 0.69 for the beams of Series III (with higher steel ratio). The strengthening ratio is shown to be inversely proportional to the steel reinforcement ratio.
- A different preloading loading history in the slabs of Series I and II (due to unloading and reloading) did not affect the flexural behavior of these slabs following strengthening.
- An increase in the preloading level resulted in a decrease in the maximum CFRP strain achieved prior to IC debonding failure.

- Although the slabs preloaded to a higher level responded to the subsequently applied loading with a higher concrete strain than corresponding slabs preloaded to a lower level, there was an undeniable strength increase for all the slabs and the strengthening allowed the slabs to regain their stiffness even after a high level of preloading. Nonetheless, the preloading level did not affect the ultimate concrete tensile strains.
- Adhesion between the CFRP laminate and the concrete has a significant effect on the slab deformation after the steel reinforcement yields. The load-induced strain in the unbonded laminates ($\varepsilon_{f,\text{test}}$) ranged from 0.0050 to 0.0069, while the bonded laminates reached strains of 0.0093 to 0.0069. Similarly, the CFRP strain efficiency ($\eta_{\varepsilon f}$) ranged from 0.68 to 0.87 for slabs strengthened with bonded laminates and from 0.56 to 0.68 for the slabs with unbonded laminates.
- Measurements of concrete strains in tension zone confirmed a significant beneficial effect of the adhesion between the laminates and the concrete. Larger concrete strains were observed in slabs strengthened with unbonded laminates.
- Despite the preload levels in some cases exceeding the serviceability limit states (and even the ultimate limit states) prior to strengthening, the application of prestressed CFRP laminates resulted in a significant reduction of deflections and strains due to subsequently applied loads and led to a recovery of slab stiffness to a value similar to that of nonpreloaded slabs.
- Preloading had negligible effects on the deflection of the strengthened slabs, which reached similar maximum deflections regardless of preload level.
- Flexural strengthening with prestressed CFRP is an efficient means of strengthening RC members carrying large loads.
- Comparison of experimental and calculated load-curvature responses for the strengthened slabs of Series III validated the analytical model presented in this work for fully bonded prestressed CFRP systems including the effects of preload prior to strengthening.

Acknowledgments

This study was carried out as part of the project, "Innovative resources and effective methods of safety improvement and durability of buildings and transport infrastructure in the sustainable development strategy," (POIG.01.01.02-10-106/09) financed by the European Union from the European Fund of Regional Development based on the Operational Program of the Innovative Economy, which the authors wish to acknowledge.

Notation

The following symbols are used in this paper:

A_i = cross-sectional area of the ith concrete layer;
A_s = cross-sectional area of the steel reinforcing bars;
A_{s1} = cross-sectional area of the tensile steel reinforcement;
A_{s2} = cross-sectional area of the compressive steel reinforcement;
a_1 = distance of the tensile steel reinforcement from the tensile edge;
a_2 = distance of the compressive steel reinforcement from the compressive edge;
d = effective depth of the steel tensile reinforcement
E_c = elastic modulus of concrete;
E_f = elastic modulus of CFRP laminate;
E_s = elastic modulus of steel reinforcement;
F = external applied load;
F_i = force in the ith concrete layer;
F_p = static preloading before and during strengthening;
F_{s1} = force in the tensile steel reinforcement;
F_{s2} = force in the compressive steel reinforcement;
F_u = ultimate load of a strengthened slab;
F_{u0} = ultimate load of an unstrengthened (reference) slab;
$f_{c,\text{cube}}$ = cube compressive strength of concrete;
$f_{ct,sp}$ = tensile splitting strength of concrete;
f_c = cylinder compressive strength of concrete;
f_y = yield strength of steel reinforcement;
f_t = ultimate tensile strength of steel reinforcement;
f_{fu} = ultimate tensile strength of CFRP laminate;
h = height of cross section;
h' = distance between levels of compressive and tensile strains measurements;
M = bending moment;
N = longitudinal (axial) force;
v = vertical displacement;
v_5 = vertical displacement at the slab midspan;
y_i = location of the ith layer of concrete;
ε_c = compressive concrete strain;
ε_{cr} = cracking strain of concrete;
ε_{cu} = ultimate concrete compressive strain;
ε_{fp} = strain due to prestressing CFRP laminate;
$\varepsilon_{f,\text{test}}$ = maximum applied load-induced tensile strain of CFRP laminate registered in the test (at slab failure);
$\varepsilon_{f,\text{tot}}$ = total tensile strain of CFRP laminate;
ε_{fu} = ultimate tensile strain of CFRP laminate;
ε_i = strain in the ith layer of concrete;
ε_{su} = ultimate tensile strain of steel reinforcement;
ε_t = average concrete strain in tension zone;
$\varepsilon_{t,\text{aver}}$ = average tensile concrete strain at the midspan of the slab measured at the depth of tensile steel reinforcement;
κ = curvature;
η_F = strengthening ratio;
$\eta_{\varepsilon f}$ = CFRP strain efficiency; and
σ_{fp} = prestressing stress level in the CFRP laminate.

References

Aram, M. R., Czaderski, C., and Motavalli, M. (2008). "Effects of gradually anchored prestressed CFRP strips bonded on prestressed concrete slabs." *J. Compos. Constr.*, 10.1061/(ASCE)1090-0268(2008)12:1(25), 25–34.

Czaderski, C., and Motavalli, M. (2007). "40-year-old full-scale concrete bridge girder strengthened with prestressed CFRP plates anchored using gradient method." *Compos. Part B*, 38(7–8), 878–886.

Czkwianianc, A., and Kaminska, M. E. (1993). *Method of nonlinear analysis of one-dimensional reinforced concrete members*, KILiW PAN IPPT, Warsaw, 36 (in Polish).

Deuring, M. (1993). "Verstärken von Stahlbeton mit gespannten Faserverbundwerkstoffen." *EMPA Dübendorf, Bericht Nr. 224*, Switzerland (in German).

El-Hacha, R., Wight, R. G., and Green, M. F. (2003). "Innovative system for prestressing fiber-reinforced polymer sheets." *ACI Struct. J.*, 100(3), 305–313.

Kałuża, M., and Ajdukiewicz, A. (2008). "Comparison of behaviour of concrete beams with passive and active strengthening by means of CFRP strips." *Archit. Civil Eng. Environ.*, 2, 51–64.

Kim, Y., Wight, R., and Green, M. (2008a). "Flexural strengthening of RC beams with prestressed sheets: Using nonmetallic anchor system." *J. Compos. Constr.*, 10.1061/(ASCE)1090-0268(2008)12:1(44), 44–52.

Kim, Y., Wight, R., and Green, M. (2008b). "Flexural strengthening of RC slabs with prestressed CFRP sheets: Development of nonmetallic anchor systems." *J. Compos. Constr.*, 10.1061/(ASCE)1090-0268(2008)12:1(35), 35–43.

Kotynia, R. (2006). "Analysis of reinforced concrete beams strengthened with near surface mounted FRP reinforcement." *Arch. Civil Eng.*, 52(2), 305–317.

Kotynia, R., Baky, H. A., Neale, K. W., and Ebead, U. A. (2008). "Flexural strengthening of RC beams with externally bonded CFRP systems: Test results and 3-D nonlinear FE analysis." *J. Compos. Constr.*, 10.1061/(ASCE)1090-0268(2008)12:2(190), 190–201.

Kotynia, R., and Kamińska, M. E. (2003). "Ductility and failure mode of RC beams strengthened for flexure with CFRPs." *Rep. 13*, Dept. of Concrete Structures TUL, Poland.

Kotynia, R., Walendziak, R., Stoecklin, I., and Meier, U. (2011). "RC slabs strengthened with prestressed and gradually anchored cfrp strips under monotonic and cycling loading." *J. Compos. Constr.*, 10.1061/(ASCE)CC.1943-5614.0000081, 168–180.

Meier, U. (1995). "Strengthening of structures using carbon fibre/epoxy composites." *Constr. Build. Mater.*, 9(6), 341–351.

Pellegrino, C., and Modena, C. (2009). "Flexural strengthening of real-scale RC and PRC beams with end-anchored pretensioned FRP laminates." *ACI Struct. J.*, 106(3), 319–328.

Stöcklin, I., and Meier, U. (2003). "Strengthening of concrete structures with prestressed and gradually anchored CFRP strips." *Proc., 6th Int. Symp. FRP Reinforcement for Concrete Structures, FRPRCS-6*, K. H. Tan, ed., World Scientific, Singapore, 1321–1330.

Teng, J. G., Chen, J. F., Smith, S. T., and Lam, L. (2002). *FRP strengthened RC structures*, Wiley, Chichester, UK.

Trintafillou, T. C., Deskovic, N., and Deuring, M. (1992). "Strengthening of concrete structures with prestressed fiber reinforced sheets." *ACI Struct. J.*, 89(3), 235–244.

Wight, R. G., Green, M. F., and Erki, M.-A. (2001). "Prestressed FRP sheets for poststrengthening reinforced concrete slabs." *J. Compos. Constr.*, 10.1061/(ASCE)1090-0268(2001)5:4(214), 214–220.

Young-Chan, Y., Ki-Sun, C., and JunHee, K. (2012). "An experimental investigation on flexural behavior of RC beams strengthened with prestressed CFRP strips using a durable anchorage system." *Compos. Part B*, 43(8), 3026–3036.

Yu, P., Silva, P., and Nanni, A. (2008). "Flexural strength of reinforced concrete beams strengthened with prestressed carbon fiber-reinforced polimer sheets—part II." *ACI Struct. J.*, 105(1), 11–20.